

# Ultrathin SiO<sub>2</sub> on Si: III Mapping the layer thickness efficiently by XPS<sup>†</sup>

M. P. Seah<sup>1\*</sup> and R. White<sup>2</sup>

<sup>1</sup> National Physical Laboratory, Teddington, Middlesex TW11 0LW, UK

<sup>2</sup> Thermo VG Scientific, The Birches Industrial Estate, Imberhorne Lane, East Grinstead, West Sussex RH19 1UB, UK

Received 2 July 2002; Revised 3 September 2002; Accepted 3 September 2002

For many electronic and other purposes, oxides in the range 2–10 nm are grown on silicon. These layers are usually monitored and measured by ellipsometry. Ellipsometry is particularly favoured because it may be integrated into semiconductor production lines, it is fast and, using optical radiation, is relatively benign. Modern ellipsometers can be used to map large wafers in detail with precisions of 0.002 nm (i.e. 0.05%). Unfortunately, it is not known if calibrations of ellipsometers, made for thicker films, can be extended down into this region. Also, unfortunately, the method does not distinguish variations in the oxide thickness from variations in the carbonaceous or water contamination overlayers that always will be present in samples exposed to the environment. Ellipsometric analysis of a 200 mm wafer with 4 nm of oxide shows a ring that may be of oxide or contamination that is 0.2 nm thicker than the central region of the wafer. By mapping with angle-resolved XPS, using a new Thermo VG Scientific Theta 300 instrument, the true aspects of this oxide profile may be verified. Improvements in the data processing of the Theta 300 probe measurements allow similar maps to those of ellipsometry to be obtained with a thickness precision of 0.01 nm (i.e. 0.2%). Crown Copyright © 2002 published by John Wiley & Sons, Ltd.

**KEYWORDS:** ellipsometry; layer thickness; SiO<sub>2</sub>; wafer homogeneity; XPS

## INTRODUCTION

Over recent years, the layer thicknesses of gate oxides for device fabrication have been progressively falling. Gate oxides are currently being fabricated at <2 nm thickness, but for SiO<sub>2</sub> layers the minimum will be set by the adventitious oxide thickness, thought to be generally slightly <1 nm and by electrical breakdown. The International Technology Roadmap for Semiconductors (ITRS)<sup>1</sup> indicates how the SiO<sub>2</sub> equivalent thickness will progressively reduce from 1.3–1.6 nm in 2001 to 0.9–1.4 nm by 2004, 0.6–1.1 nm by 2007 and 0.4–0.5 nm by 2016. These are required with a thickness control of ~1% at one standard uncertainty. Historically, the industry has achieved most items ahead of the ITRS deadline. This reduction cannot be achieved in SiO<sub>2</sub> and so other materials or layer structures will be used. It is unlikely that layers much below 1 nm will be used but the layers may be of graded or other mixed compositions.

The industry has used ellipsometry in the past for measuring oxide film thicknesses. The ellipsometers have been calibrated using reference data and checked using certified reference materials.<sup>2,3</sup> However, these materials have a minimum thickness of 10 nm and the certificates

warn that, for these thinner oxides, contamination layers accumulate and need to be removed by a defined cleaning procedure.<sup>3</sup> Ellipsometers have not been calibrated in the lower thickness region down to 1 nm but users hope that the calibration may be extended downwards. Recent tests by Cole *et al.*<sup>4</sup> indicate a typical discrepancy between ellipsometry and x-ray photoelectron spectroscopy (XPS) of 6% for thicknesses of >10 nm but rising to 50% at 5 nm and a factor of four different at 1 nm.

Ellipsometry will continue to find significant favour because the instruments are simple to use, fit easily with production lines and can provide maps of large wafers in a 50 × 50 array with 0.002 nm precision in a relatively short time. However, the layer measurements give a weighted sum of the thicknesses of the oxide, any carbonaceous contamination and any adsorbed water layer. For the 2 nm oxides these extra contaminations may add significantly to the measured thickness. Recent work in ellipsometry has used warmed samples, which reduces the water adsorption but cannot remove the carbonaceous contamination<sup>5</sup> or the final layer of water. On the other hand, XPS can be used to measure the thickness of the SiO<sub>2</sub> layer under any normal contamination layer without being affected significantly.<sup>6</sup> Furthermore, because the oxide is changed by grading with other elements or to other components or multilayers, it is only XPS that is non-destructive and has the separation of information for the various elements and the composition as a function of depth capability.<sup>7</sup> However, XPS is both slower and less precise than ellipsometry. In the present work we

\*Correspondence to: M. P. Seah, Centre for Optical and Analytical Measurement, National Physical Laboratory, Teddington, Middlesex TW11 0LW, UK. E-mail: martin.seah@npl.co.uk  
Contract/grant sponsor: UK Department of Trade and Industry.

<sup>†</sup>Presented at the Twelfth International Conference on Surface and Nanoanalysis (QSnA-12), University of Surrey, UK, 8–11 July 2002.

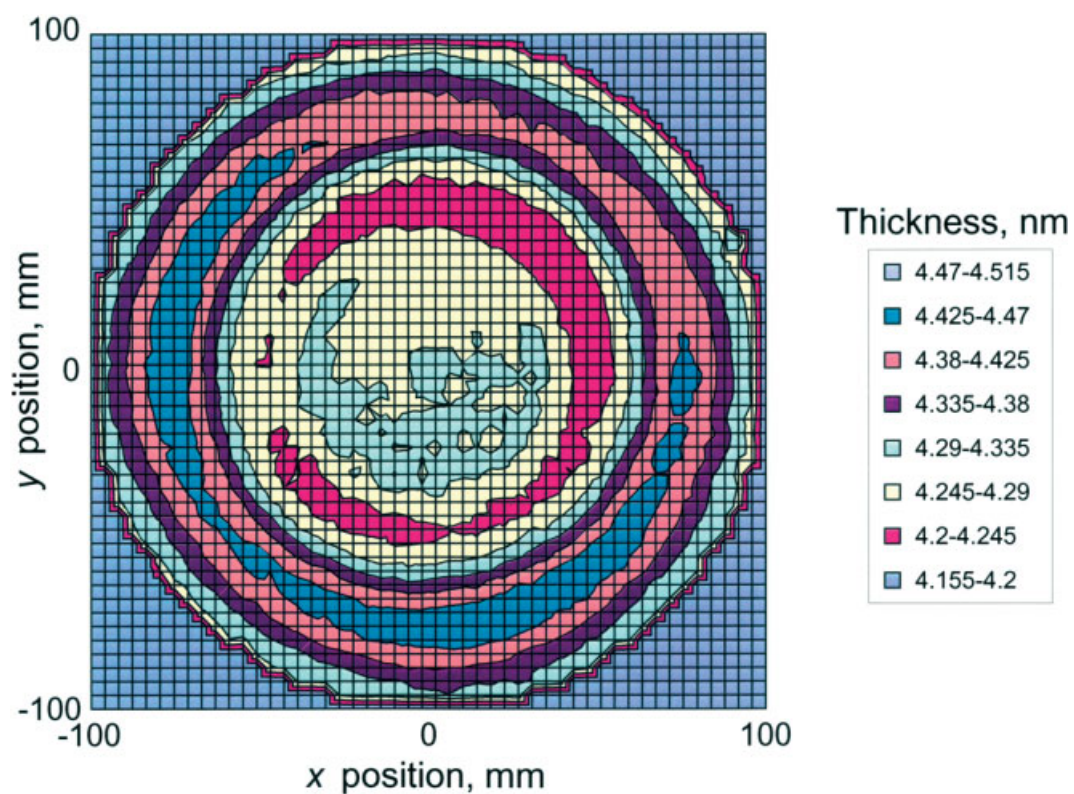


**Plate 1.** Thickness data from the Philips PZ2000 ellipsometer used to produce a map with contours at 1% intervals.

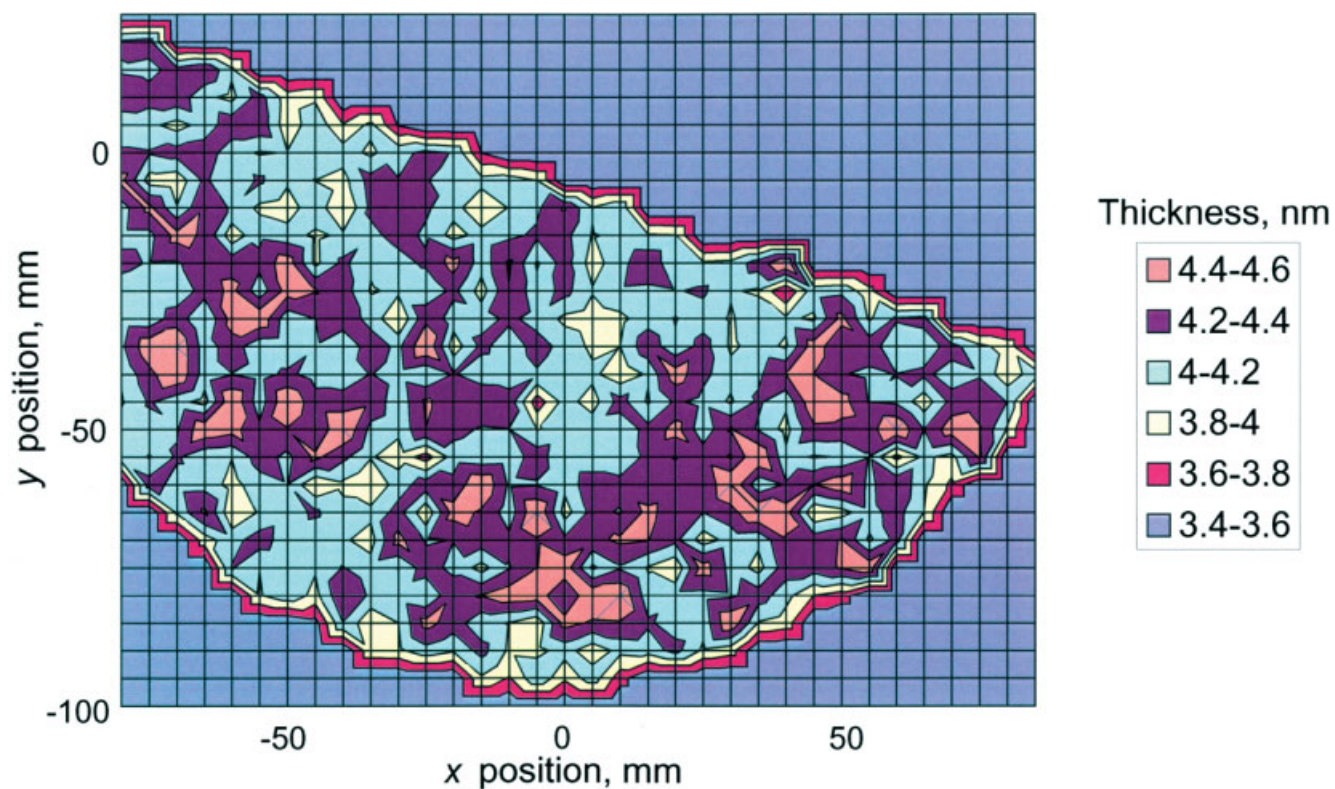


**Plate 2.** Map of a portion of the wafer shown in Plate 1 analysed by XPS using the gradient of the  $\ln(1 + R_{\text{expt}}/R_0)$  vs.  $\sec \theta$  plot for  $\theta \leq 60^\circ$ .

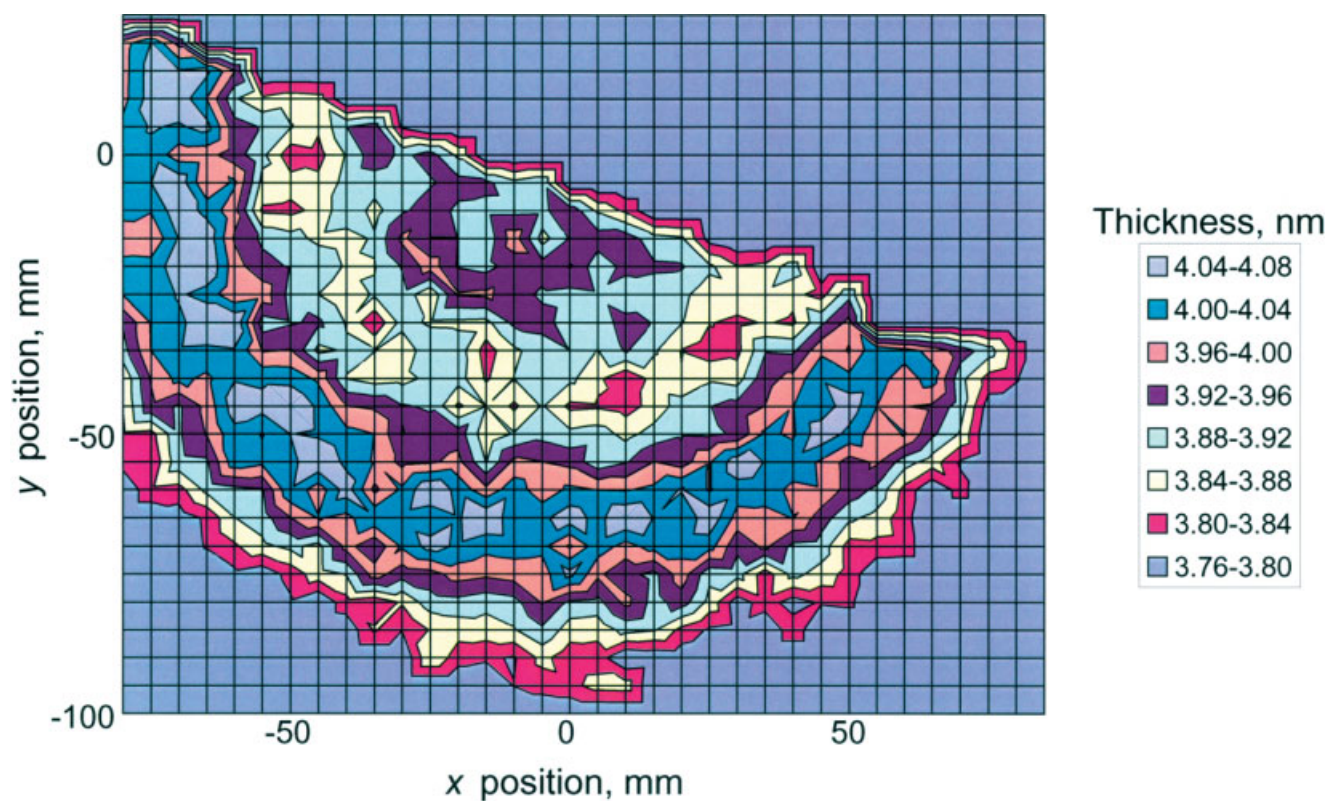


**Plate 3.** Map of Plate 1 but for the average value of  $d_{\text{oxide}}$  for  $20^\circ \leq \theta \leq 60^\circ$  obtained directly.

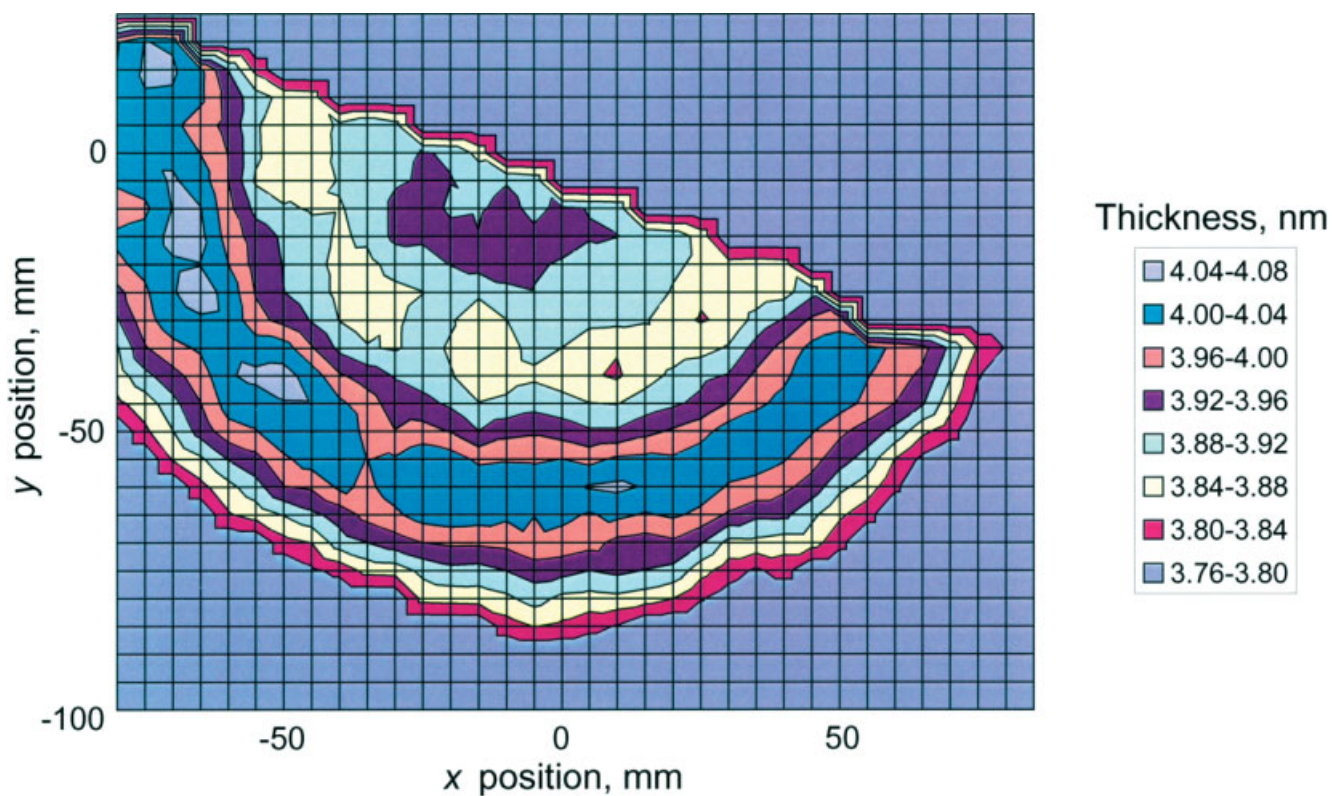


**Plate 4.** Map of Plate 3 but with a nearest-neighbour smooth.

investigate the level of precision available in mapping wafers by XPS using a new instrument specifically designed for this purpose. We do not address the accuracies here because these are more complex and will be dealt with in a later paper<sup>8</sup> in this series.<sup>5,6</sup>

## EXPERIMENTAL

As part of other work, a number of 200 mm Si(100) wafers were prepared and oxidized to form oxides of thicknesses in the range 2–5 nm. One of these, not selected for the other work, is used here. It was selected on the basis of the apparent unevenness of the oxide thickness as measured by ellipsometry.

The ellipsometric measurements in this work were conducted using a Philips PZ2000 ellipsometer designed for clean room operation. This is an instrument designed to work as a metrology tool on a semiconductor fabrication line. It is highly automated and can handle batches of wafers rapidly and efficiently. It employs an HeNe laser of 632.8 nm wavelength, incident at 70° from the surface normal. Wafers from the production line were placed in Fluoroware wafer carriers and sealed in double polyethylene bags in the clean room for transit to the ellipsometer, which was at a separate facility. The bags and containers were opened in the new clean room and wafers were inserted automatically into the ellipsometer for measurement. This process should have kept the carbonaceous and particulate contamination to a minimum,<sup>5</sup> although such contamination will always be present to some extent.

The 200 mm wafer used in this study was cut into three pieces, two of which were D-shaped with widths of 95 mm and one, across the centre, of 10 mm width. One of the D-shaped pieces was used for the present XPS measurements. All cuts were made by scribing along [110] directions. In accordance with the recommendations that we have established elsewhere,<sup>6</sup> to reduce the effects of forward focusing, which change the intensities of the silicon substrate along low index directions, the measurements were recorded with the analyser in an azimuth set at 22.5° between the [011] and [010] azimuths of the wafer. This was done by setting the straight edge of the D shape normal to the analyser azimuth and then rotating it 22.5° clockwise as viewed from above. The XPS measurements were conducted in a Thermo VG Scientific Theta 300 instrument that records spectra over the range of emission angles from 23° to 83° simultaneously and which has a translation stage to form maps of spectra. The photoelectron spectra were generated using Al K $\alpha$  radiation in a monochromator operating at 100 W with a spot size of 400  $\mu$ m. With this spectrometer, the spectra may be recorded at 0.625° angular intervals, but to reduce the size of the data files the range 23–83° was split into 16 intervals, each of 3.75°. This provided 16 spectra of 112 energy channels from 90.77 to 111.23 eV binding energy at 0.1827 eV energy intervals for each point in the map. The map was formed by an array of 26 steps in the *y*-direction and 34 in the *x*-direction at 5.11 mm displacements. In all, a total 14 144 spectra, from the 884 mapping points, were collected in 36 h over a weekend. To obtain good intensity levels, a spectrometer nominal

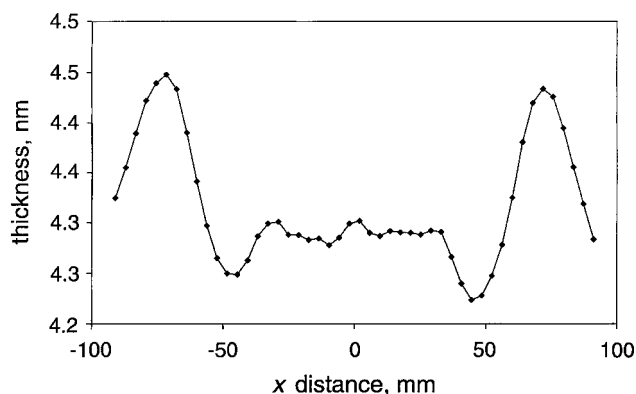
resolution of 1.4 eV was used. The data were processed for curve fitting using the VG Advantage software (version 1.62) in which the user sets up the fitting on one spectrum and this is then applied automatically to the remaining 14 143 spectra. The total fitting process takes ~1 min.

Prior to the peak synthesis, the spin-orbit splitting of the Si 2p<sub>3/2,1/2</sub> pair was removed by subtracting an intensity of 50% for each channel at 0.60 eV higher binding energy.<sup>9</sup> The Si peak areas for the elemental and oxide states then were exported to an Excel spreadsheet for further data analysis.

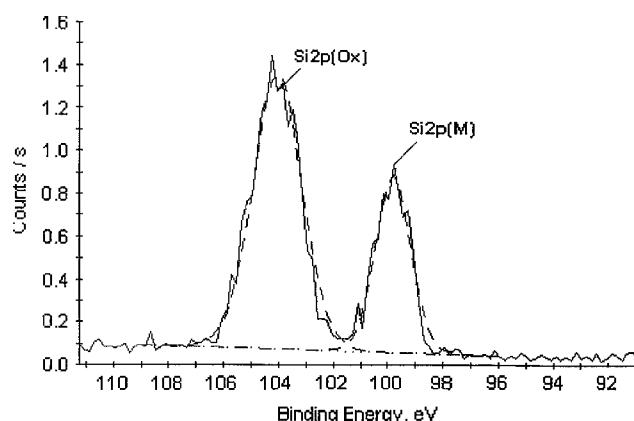
## RESULTS

Plate 1 is a map of thicknesses derived from the ellipsometric data. This shows a wafer with an oxide thickness typically of 4.3 nm that varies from 4.25 nm in the centre, through a ring of thickness 4.45 nm and falls back again to 4.25 nm. It was not clear from these data if the ring with an excess height of 0.2 nm (4.7% relative) was real or arose from a ring of contamination. Figure 1 shows a trace across the wafer and it is clear from these data that the ellipsometric precision is better than 0.002 nm and is probably close to 0.001 nm (0.02% relative).

Data from the Thermo VG Scientific Theta 300 instrument give the intensities of the Si 2p peak in the elemental (*I*<sub>Si</sub>) and oxide (*I*<sub>SiO<sub>2</sub></sub>) states as shown in Fig. 2. A straight-line



**Figure 1.** An x-linescan across the centre of the wafer of Plate 1.



**Figure 2.** One of the 14 144 spectra from the Thermo VG Theta 300 instrument at 24.88° emission angle and 150 s acquisition time.

background was removed using averaging of the end points at 95.93 and 109.02 eV over 0.92 eV. A Shirley background<sup>10</sup> may be used but here the data differed by <1%. In the rest of the work in this series published elsewhere,<sup>5,6</sup> the Shirley background is always used unless explicitly stated. The above analysis gave a set of intensities as a function of the emission angle  $\theta$ , which may be used to deduce the oxide thickness in the relation<sup>6</sup>

$$d_{\text{oxide}} = L_{\text{SiO}_2} \cos \theta \ln(1 + R_{\text{expt}}/R_0) \quad (1)$$

where

$$R_{\text{expt}} = I_{\text{Si}}/I_{\text{SiO}_2} \quad (2)$$

and where  $L_{\text{SiO}_2}$  is the attenuation length of the Si 2p electrons in the oxide overlayer and  $R_0$  is the ratio of the Si 2p elemental and oxide intensities for infinitely thick bulk materials. It is assumed here that  $L_{\text{SiO}_2}$  is a constant, although this is only correct to within ~2% for  $\theta \leq 60^\circ$ .<sup>11,12</sup> Elsewhere,<sup>6</sup> we give a recommended value of  $L_{\text{SiO}_2}$  for Al K $\alpha$  x-rays as 3.448 nm with the main uncertainty, thought to be 10%, arising from the calculations for the inelastic mean free path involved.<sup>13</sup> The value of  $R_0$  varies between different sources in the literature and these are reviewed by Seah and Spencer.<sup>6</sup> Further experimental data provide a recommended value of

$$R_0 = 0.9329 \pm 0.0227 \quad (3)$$

for the reference geometry,<sup>6</sup> where the uncertainty is the standard uncertainty. This value of  $R_0$  is higher than is generally used and is appropriate for a Shirley background subtraction rather than a straight line. As can be seen from Fig. 2, there will be very little difference.

In the Avantage software, a least-squares fit is made to a plot of  $\ln(1 + R_{\text{expt}}/R_0)$  versus  $\sec \theta$  to give a gradient of  $d_{\text{oxide}}/L_{\text{SiO}_2}$  and hence a value of  $d_{\text{oxide}}$  for each pixel of the map. The result of this direct procedure is given in Plate 2. This map is good and gives a mean thickness of 3.9 nm with a scatter of 4.7%. Unfortunately, as noted above, the ring height is only 4.7% and so is almost swamped by the noise in the data.

The method used in Avantage software ignores the fact that the plot should go through the origin if we know that the film is of an even thickness. Hence, we are determining a gradient and an offset where the offset is small but actually should be zero. The uncertainty in the offset leads to unwanted noise in the gradient and hence in  $d_{\text{oxide}}$ . If we generate this plot using the average of the data from the central region, we get the result shown in Fig. 3. It is clear that the plot of  $\ln(1 + R_{\text{expt}}/R_0)$  vs.  $\sec \theta$  is linear for  $\theta \leq 60^\circ$  but the intensity falls below that expected for higher angles based on Eqn. (1). This is expected and arises as a result of elastic scattering.<sup>11,12</sup> The concept of Eqn. (1) is not useful beyond  $60^\circ$ . Plate 2 thus only uses data for  $\theta \leq 60^\circ$ . If we now try to calculate  $d_{\text{oxide}}$ , not from the gradient of this plot but from each angular measurement using Eqn. (1) directly, we get 16 values of  $d_{\text{oxide}}$ , 10 of which are for  $\theta \leq 60^\circ$ , as shown in Fig. 4. These thicknesses are not all the same because the  $I_{\text{Si}}$  part of Eqn. (1) is affected by forward focusing.

The geometry chosen here minimizes the effect, as shown in our earlier work.<sup>(6)</sup> The plot found there, for a thinner oxide, using a smaller angular acceptance in the azimuthal direction is shown dotted for comparison. This has been scaled by a factor to adjust for the different thicknesses, and is for illustration purposes only. The value of  $R_0$  given in Eqn. (3) is for the  $35^\circ$  emission orientation in this azimuth, and is very close to the mean obtained here by averaging the  $d_{\text{oxide}}$  values for all angles  $\leq 60^\circ$ . Thus, from each out of the angle data we obtain one value of  $d_{\text{oxide}}$  by this method, as we did from the gradient previously. For oxide points evenly populated over the range  $1 \leq \sec \theta \leq 2$ , this would lead to an improvement in the uncertainty of  $d_{\text{oxide}}$  by a factor of 6. This reduces the uncertainty in the thickness to a value that is less than the ring height; Plate 3 shows this result.

The ring is now very clearly visible and the scatter is close to the 0.5% value expected. We may smooth this result further by using a simple matrix of 0.3333 of the intensity of a given pixel with 0.1667 of the intensity of the four adjacent pixels, which we term a nearest-neighbour smooth. This leads to a further improvement of  $\sqrt{4.5}$  in the uncertainty of  $d_{\text{oxide}}$ , as shown in Plate 4. Thus, the overall improvement is now a factor of 12.7. In Fig. 5 we show linescans across this map as a pair of chords with

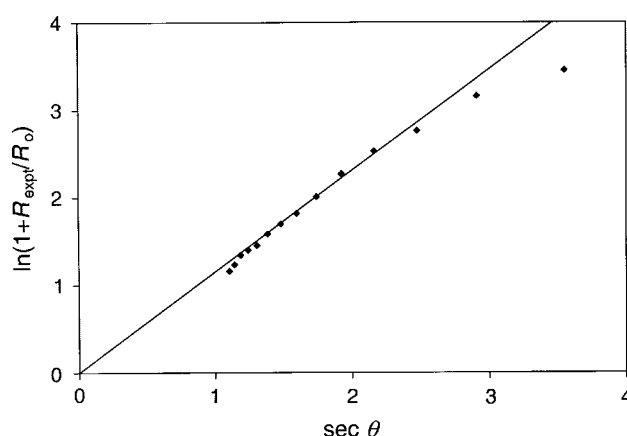


**Figure 3.** Plot of  $\ln(1 + R_{\text{expt}}/R_0)$  vs.  $\sec \theta$  for the data from the central region of the wafer shown in Plate 2.

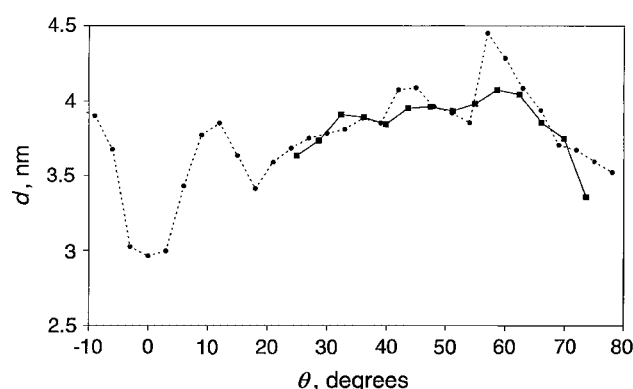


**Figure 4.** Values of  $d_{\text{oxide}}$  deduced from Eqn. (1) for each of the angles for the central region of the wafer shown in Plate 2. Also shown dotted are the data in this azimuth for a thinner oxide,<sup>6</sup> scaled up by a factor of 5.1 for illustration purposes.

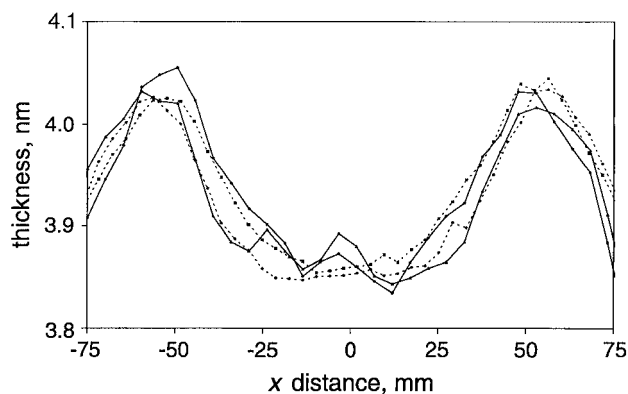


**Figure 5.** Chords through the data at 40 nm from the wafer centre and in the x-directions of Plates 1 and 4 for ellipsometry (---) and XPS (—), respectively. The ellipsometric data have been scaled down by a factor of 1.1 for comparison.

a similar pair from the ellipsometric data. In Fig. 5, we have simply scaled the ellipsometric data down by a factor of 1.1 to match the XPS data. At the present time, we have not calibrated the ellipsometer to be accurate in this thickness range and have simply used the manufacturer's calibration appropriate for thicker layers. The accuracy of these data is the subject of further work in this series. It is clear that the XPS scatter now has a standard deviation of  $\sim 0.25\%$  or 0.01 nm. This is more than adequate to observe the structure seen in the ellipsometry. Note that the chords are not quite overlapping. They are all at 40 nm from the centre of the wafer but the XPS chord is rotated  $22.5^\circ$  anticlockwise relative to the ellipsometry data. The ellipsometric data are essentially rotationally symmetric and so this is not a significant issue. The small increase in thickness in the ring at a radius of 50 mm in the ellipsometry data of Plate 1 is repeated but rotated  $22.5^\circ$  clockwise in the XPS data of Plate 4. The XPS and ellipsometric data here match excellently and show that XPS can be a powerful alternative for ellipsometry in cases where the ellipsometry has insufficient information to address the variations in thickness of more than one material.

## CONCLUSIONS

Mapping of the SiO<sub>2</sub> thicknesses on wafer surfaces using XPS may be made with good precision. Provided that the SiO<sub>2</sub> overlayer is of a uniform material, the most effective way of deriving the thickness is to use the data for all angles of emission up to  $60^\circ$  from the surface normal. The thickness data are calculated for each of the 10 angles in this range, using Eqn. (1), and then are averaged to give one  $d_{\text{oxide}}$  value at each pixel. This leads to an improvement in the signal quality by a factor of six so that, by recording data over 36 h, a map of 884 mapping points may be obtained with a thickness precision of 0.5%. With a very simple smoothing algorithm, this is improved further to 0.25%. Values given for the critical parameters  $L_{\text{SiO}_2}$  and  $R_0$  in Eqn. (1) are  $3.448 \pm 0.34$  nm and  $0.9329 \pm 0.0227$ , which are the best currently available. These will be revised in further work.

## Acknowledgements

The authors would like to thank Neil Lloyd for the ellipsometry data, S. J. Spencer for some of the data processing and P. J. Cumpson for organizing the ellipsometry measurements. This work forms part of the Valid Analytical Measurement Programme of the National Measurement System Policy Unit of the UK Department of Trade and Industry.

## REFERENCES

1. *International Technology Roadmap for Semiconductors* (2001 edition). <http://public.itrs.net/>.
2. BCR-564, IRMM, Dr. J Pauwels. IRMM: Geel, Belgium.
3. *NIST Ellipsometry SRMs 2531 to 2536*. Office of Reference Materials, NIST: Gaithersburg, MD 20899, USA.
4. Cole DA, Shallenberger JR, Novak SW, Moore RL, Edgell MJ, Smith SP, Hitzman CJ, Kirchhof JF, Principe E, Nieveen W, Hueng FK, Biswas S, Bleiler RJ, Jones K. *J. Vac. Sci. Technol. B* 2000; **18**: 440.
5. Seah MP, Spencer SJ. *J. Vac. Sci. Technol. A*, in press.
6. Seah MP, Spencer SJ. *Surf. Interface Anal.* 2002; **33**: 640.
7. Cumpson PJ. *J. Electron Spectrosc.* 1995; **73**: 25.
8. Seah MP, Spencer SJ. to be published.
9. Hollinger G, Himpell FJ. *Appl. Phys. Lett.* 1984; **44**: 93.
10. Shirley DA. *Phys. Rev. B* 1972; **5**: 4709.
11. Cumpson PJ, Seah MP. *Surf. Interface Anal.* 1997; **25**: 430.
12. Powell CJ, Jablonski A. *J. Electron Spectrosc.* 2001; **114–116**: 1139.
13. Tanuma S, Powell CJ, Penn DR. *Surf. Interface Anal.* 1991; **17**: 911.